

## Research Article

Received: 8 January 2022

Revised: 10 May 2022

Accepted article published: 16 May 2022

Published online in Wiley Online Library: 7 June 2022

(wileyonlinelibrary.com) DOI 10.1002/jctb.7134

# Complete wastewater discoloration by a novel peroxidase source with promising bioxidative properties

Natalia Klanovicz,<sup>a,b\*</sup>  Fábio Spizza Stefanski,<sup>b</sup>  Aline Frumi Camargo,<sup>b,c</sup>  William Michelon,<sup>d</sup>  Helen Treichel<sup>b</sup>  and Antonio Carlos Silva Costa Teixeira<sup>a</sup> 

## Abstract

**BACKGROUND:** Our study aimed to characterize and prospect immobilization strategies for a novel fungal peroxidase (POD) and insert it in pollutant remediation context. The enzymatic extract was obtained by submerged fermentation of *Trichoderma koningiopsis* in an alternative substrate consisting of fresh microalgal biomass. The immobilization efficiency was evaluated by monitoring the residual activity (RA) and the discoloration potential (DP) of a synthetic dye solution. Concomitantly, the POD catalytic properties were explored, and the most promising storage strategy to maintain the enzymatic activity was studied.

**RESULTS:** The novel and non-purified guaiacol peroxidase from *T. koningiopsis* expressed a specific activity of up to 7801 U mg<sup>-1</sup> in the free form, showing stability when subjected to up to 80 °C in a pH range between 4.0 and 8.0. Furthermore, the bioproduct immobilized on Fe<sub>3</sub>O<sub>4</sub> magnetic nanoparticles, named magnetic nanozymes (MN-POD), expressed up to 689% RA and 100% removal for the Direct Brown 27 dye. An increase in the enzymatic activity, in both free and immobilized forms, was also observed after storage for up to 8 months. The synthesized magnetic nanozymes showed good reusability, maintaining 13 546 U mg<sup>-1</sup> after 10 cycles, and removing 94% of color in a second batch. Toxicological evaluation with *Allium cepa* indicated that the enzymatic discoloration process with immobilized POD was essential for eliminating genotoxic effects.

**CONCLUSION:** The *T. koningiopsis* peroxidase production and immobilization presented in this work are promising for the enzyme market and for wastewater treatment technologies due to their high bioxidative potential.

© 2022 Society of Chemical Industry (SCI).

**Keywords:** catalytic processes; degradation; environmental biotechnology; immobilization; toxicity

## BACKGROUND

As part of the subclass of organic chemical compounds known as emerging pollutants, synthetic dyes have been in the environment for a long time. Nonetheless, their impacts on human and environmental health have only been recognized recently. Their aromatic and highly complex structures make them resistant to degradation processes, as well as to light and ultraviolet irradiation.<sup>1</sup> Furthermore, it is estimated that the textile industry alone generates around 4500 million kiloliters of wastewater per year,<sup>2</sup> with a significant amount (10–15%) of the total dyes used by this industry being continuously discharged into the environment.<sup>3</sup>

Since conventional wastewater treatment systems show a limited capacity to remediate these contaminants, alternative removal or remediation methods are required. In this context, enzymatic processes have been developed with catalytic and oxidative properties capable of biotransforming persistent pollutants. These properties put the global enzyme market in constant expansion, with projections of 3.4% annual growth between 2020–2027;<sup>4</sup> this means that enzymes are starting to compete with chemical catalysts. Therefore, there is a growing interest in new enzyme sources and low-cost upstream processes that will

enable the use of enzymes as environmentally and economically viable biocatalysts.<sup>5</sup>

In the wastewater treatment sector, the oxidoreductase enzymes laccase – Lac (EC 1.10.3.2) and peroxidase – POD (EC 1.11.1.7), both of which are mainly obtained from fungi, have been explored for emerging pollutant degradation.<sup>6,7</sup> These

\* Correspondence to: N Klanovicz, Department of Chemical Engineering, Escola Politécnica, University of São Paulo, São Paulo 05508080, Brazil. E-mail: nataliaklanovicz@gmail.com

a Research Group in Advanced Oxidation Processes (AdOx), Department of Chemical Engineering, Escola Politécnica, University of São Paulo, São Paulo, Brazil

b Laboratory of Microbiology and Bioprocesses (LAMIBI), Federal University of Fronteira Sul, Erechim, Brazil

c Graduate Program in Biotechnology and Bioscience, Federal University of Santa Catarina, Florianópolis, Brazil

d Graduate Program in Civil, Sanitary and Environmental Engineering, University of Contestado, Concórdia, Brazil

enzymes have shown competitive advantages with chemical catalysts, such as performance in mild environmental conditions, low damage to the environment, and high specificity with pollutants.<sup>8</sup> However, it is essential to emphasize some of the challenges surrounding enzymatic application in contaminants removal, mainly the need to keep the reactions stable and favorable to obtain the maximum catalytic performance.

These challenges can be overcome with noncommercial enzymes, which are highly stable under extreme pH and temperature conditions and are also economically advantageous. In addition, enzymatic manipulation by immobilization is an exciting strategy to avoid enzymatic denaturation or inhibition and to enhance catalytic action, stability, and reuse by several cycles. Promising results in laccase and peroxidase immobilization have been reported using organic supports (such as carbon, synthetic polymers, chitosan, and sodium alginate) and inorganic supports (such as silica, clay, and metal oxides).<sup>5,9</sup> Different strategies have also promoted contact between the support and enzymes: these strategies include traditional encapsulation and adsorption, as well as novel techniques that synthesize magnetic nanozymes.<sup>10</sup> According to Shakerian *et al.*,<sup>9</sup> the principles of these strategies have not changed considerably in recent years, and the focus of immobilization studies remains mostly on prospecting supports and operational parameters.

In this way, enzymatic immobilization opens interesting possibilities for the development of novel technologies both for the enzyme market and the wastewater treatment sector, considering no universal protocols have been established for these processes.<sup>11</sup> Morsi *et al.*<sup>6</sup> emphasize that processes with Lac and POD to remove emerging pollutants from wastewater have been carried out primarily with high-cost commercial enzymes or after their purification and immobilization. These upstream steps increase catalytic efficiency but compromise the economical viability of enzymatic processes for dye remediation.

In this sense, the present work aims to study the immobilization strategies of a novel noncommercial and non-purified peroxidase, obtained through *Trichoderma* submerged fermentation supplemented exclusively by microalgal biomass, and evaluate its catalytic and toxicological performance in free and immobilized forms for synthetic dye discoloration.

The immobilization strategies chosen were: (i) encapsulation in Ca-alginate beads, (ii) adsorption on commercial montmorillonite and residual rock powder, and (iii) incorporation into magnetic  $\text{Fe}_3\text{O}_4$  nanoparticles by alkaline co-precipitation. The biooxidative potential of free and immobilized fungal peroxidase was evaluated by using the dyes Direct Red 9, Direct Blue 16, Direct Yellow 27, and Direct Brown 27 as model compounds to be degraded.

## MATERIALS AND METHODS

### Enzymatic extract obtention

The enzymatic extract was produced by a submerged fermentation process using *Trichoderma koningiopsis* MK860714, supplemented with microalgal biomass, both from noncommercial sources.

The fungus is cultivated by the Laboratory of Microbiology and Bioprocesses, in a partnership with the Laboratory of Agroecology (Federal University of Fronteira Sul, Erechim, Brazil). It was isolated from the weed *Digitaria ciliaris*, out of soybean and corn cultivation areas in southern Brazil.<sup>12</sup> The microorganism growth occurred on Potato Dextrose Agar (PDA), and it was maintained

in a bacteriological greenhouse at 28 °C for 7 days before the start of fermentation.

The *Chlorella* spp. microalgal biomass was cultivated and kindly provided by Embrapa Swine and Poultry (Concórdia, Brazil). Its cultivation occurs in a biological reactor with the aim of removing ammonia and phosphorus from swine wastewater digestate by phytoremediation. The biomass is composed of 56% protein, 35% carbohydrates, 2% lipids, and 7% minerals.<sup>13</sup>

Fermentation was carried out in an Erlenmeyer with a practical volume of 100 mL under the conditions previously optimized by Stefanski *et al.*<sup>14</sup> to produce the target enzymes. The medium consisted of 10 g of fresh microalgal biomass (89% humidity) and 90 mL of distilled water. The Erlenmeyer was autoclaved at 120 °C and 1 atm for 20 min, after which the medium was inoculated with 10 mL of a suspension containing  $10^6$  spores of *T. koningiopsis* per milliliter. The spore's suspension was obtained by adding 100 mL of Tween 80 solution (0.1% v v<sup>-1</sup>) to the Erlenmeyer containing the microorganism. Then, 0.1 mL of the Erlenmeyer content was used for spore counting using a Neubauer chamber (Fuchs Rosenthal Net-line, New Optics) and the Olympus CX21 Biological Microscope.

The fermentation was conducted for 72 h in an orbital shaker (New Brunswick™, Germany) at 120 rpm and 28 °C. After fermentation, the Erlenmeyer content was filtered to remove the fungal and microalgal biomass, and the liquid permeate was centrifuged (NT 815 - NovaTecnica, Brazil) at 2000 rpm and 4 °C for 10 min. The supernatant corresponds to the enzymatic extract, and the rest of the fermentation content was sterilized and discarded.

### Enzymatic activity quantification

All the assays described in the present work were performed with the non-purified supernatant called enzymatic extract. The quantified oxidoreductase enzymes were guaiacol peroxidase, with methodology adapted from Garda-Buffon *et al.*,<sup>15</sup> and laccase, adapted from Hou *et al.*<sup>16</sup>

For peroxidase, 1 mL of extract was mixed with 1.5 mL of sodium phosphate buffer pH 5.5 (5 mmol L<sup>-1</sup>), 0.5 mL of the substrate guaiacol (93 mmol L<sup>-1</sup>), 1 mL of the cosubstrate hydrogen peroxide (75 mmol L<sup>-1</sup>), and 2 mL of distilled water.

The U unit of peroxidase specific activity was defined as the enzyme amount capable of causing a 0.001 increase in the absorbance unit per minute per milligram of total protein, when incubated at 25 °C for 10 min and read in a spectrophotometer (UV-M51-Bel, Italy) at 470 nm. Total protein concentration was quantified by the Bradford method,<sup>17</sup> and specific activity was expressed in U mg<sup>-1</sup>, dividing the enzymatic activity (U mL<sup>-1</sup>) by the protein concentration (mg mL<sup>-1</sup>) of the sample.

For laccase, 0.2 mL of extract was added to the reaction medium containing 0.4 mL of 2,2'-azino-di-(3-ethylbenzothiazolino-6-sulfonic acid) (ABTS), along with 10 mmol L<sup>-1</sup> and 3.4 mL of sodium acetate buffer pH 4.8 (50 mmol L<sup>-1</sup>). After incubation for 5 min at 40 °C, the substrate oxidation was monitored by absorbance read in a spectrophotometer at 420 nm ( $\epsilon_{420} = 36\,000\text{ L mol}^{-1}\text{ cm}^{-1}$ ). The U unit of laccase was defined as the enzyme amount capable of oxidizing 1 μmol of substrate per minute.

### Discoloration studies

Preliminary discoloration studies were carried out with four commercial synthetic dyes (Guarany Ind. Ltda., Brazil) to verify the affinity between enzyme and dye structure, and the relationship between enzyme amount and discoloration potential (DP).

The dyes studied were red (455 nm), blue (595 nm), yellow (414 nm), and brown (530 nm). Their catalog names, molecular structures, and properties of interest are given in Table 1. The tests were conducted according to previous studies.<sup>18</sup> The dye solution, prepared with distilled water at 100 mg L<sup>-1</sup>, was treated with 5 or 10 mL of crude enzymatic extract and 40 mg L<sup>-1</sup> of hydrogen peroxide 35% v<sup>-1</sup>.

Crude extracts with different peroxidase:laccase ratios, obtained in previous studies with varying operational parameters in fermentation,<sup>14</sup> were applied to the dye removal study. The discoloration tests were carried out at a volume of 100 mL under constant agitation (160 rpm) and temperature (25 °C) for 5 h. The DP was quantified by the difference between initial ( $A_{bs_i}$ ) and final ( $A_{bs_f}$ ) absorbances of the treated samples (Eqn (1)).

$$DP (\%) = \frac{A_{bs_i} - A_{bs_f}}{A_{bs_i}} * 100 \quad (1)$$

### Investigation of the peroxidase activity behavior

Initially, the reaction conditions and the substrate:enzyme ratio influence on enzymatic activity were evaluated. The effect of substrate (0.5–1.0 mL) and cosubstrate (0.5–1.0 mL) concentrations in the reaction medium, and the impact of pH (4.0–8.0) and incubation temperature (20–80 °C) were studied by the Plackett-Burman experimental design, which was conducted with eight trials and three replicates under central point conditions.

Then, setting the conditions to the most favorable trial of the design, the behavior of specific activity, pH, and oxidation-reduction potential (ORP) were monitored over time to understand the catalytic cycle of the peroxidase oxidation reaction.

Additionally, crude extract samples were stored, protected from direct sunlight, under three different conditions: at room temperature (ranging between 18–28 °C), in the refrigerator (4 °C), and in the freezer (–10 °C). The residual activity (RA) monitoring was carried out in 15, 30, 60, 90, 170, and 400 days and calculated by Eqn (2), in which  $SA_i$  and  $SA_f$  correspond to the pre- and post-storage specific activity, respectively. The kinetic parameters half-life time ( $t_{1/2}$ ) and thermal denaturation constant ( $k_d$ ) were also evaluated in this study, based on a semi-natural logarithmic graph of RA as a function of storage time.<sup>19</sup>

$$RA (\%) = \frac{SA_f}{SA_i} * 100 \quad (2)$$

### Propection techniques for enzymatic immobilization

The *T. koningiopsis* enzymatic extract was submitted to three different immobilization strategies (Table 2), and their efficiency was measured by residual activity and discoloration potential.

The RA was calculated by Eqn (2), but in this case,  $SA_i$  and  $SA_f$ , respectively correspond to the specific activity of free and immobilized peroxidase. The contents retained in both the immobilization supports and the permeate were subjected to enzymatic quantification.

Preliminary tests were conducted to monitor the immobilized enzyme activity after storage at room temperature. In addition, the recovery and reuse potential of MN-POD was first assessed in two ways: (i) by activity after 10 catalytic cycles, renewing the peroxidase reaction medium described in section 'Investigation of the peroxidase activity behavior'; and (ii) by a new decolorization batch, according to the procedure detailed in section 'Decoloration studies'. The MN-POD recovery was made by the commercial magnet NdFeB (N45).

### Encapsulation in Ca-alginate and modified Ca-alginate beads

The immobilization in beads was tested in two ways: in the presence and absence of the enzyme-substrate and cosubstrate. In both cases, the methodology was adapted from Rezvani *et al.*,<sup>20</sup> according to which, initially, a gel was prepared with sodium alginate and distilled water (1.75% w v<sup>-1</sup>). In this step, the addition of 0.08% hydrogen peroxide and 1% guaiacol to the gel was tested, both in a proportion corresponding to the reaction medium of the enzymatic activity measurement.

The enzymatic extract was then added to the gel (6.7% v v<sup>-1</sup>). After homogenization, it was dripped with a peristaltic pump (20 mL min<sup>-1</sup>) to 100 mL of a calcium chloride solution (4.5% w v<sup>-1</sup>) and kept in an ice bath under constant magnetic stirring.

The beads formed in the previous procedure were kept immersed in the calcium chloride solution for 20 min at 4 °C. Next, a sieve was used to retrieve the beads, which were then thoroughly washed with distilled water, thus obtaining the POD- and ModPOD-beads samples.

**Table 1.** Catalog name, molecular formula, and properties of the dyes used in discoloration experiments by enzymatic biocatalysis

Commercial name	Catalog name	Formula	Molar weight (g mol <sup>-1</sup> )	Molecular structure
<b>Red dye</b>	Direct Red 9	C <sub>34</sub> H <sub>19</sub> ClN <sub>8</sub> Na <sub>4</sub> O <sub>12</sub> S <sub>4</sub>	987.2	
<b>Blue dye</b>	Direct Blue 16	C <sub>32</sub> H <sub>20</sub> N <sub>5</sub> Na <sub>3</sub> O <sub>11</sub> S <sub>3</sub>	815.7	
<b>Yellow dye</b>	Direct Yellow 27	C <sub>25</sub> H <sub>20</sub> N <sub>4</sub> Na <sub>2</sub> O <sub>9</sub> S <sub>3</sub>	662.6	
<b>Brown dye</b>	Direct Brown 27	C <sub>39</sub> H <sub>24</sub> N <sub>7</sub> Na <sub>3</sub> O <sub>9</sub> S <sub>2</sub>	867.7	

**Table 2.** Strategies prospected to immobilize *T. koningiopsis* peroxidase

Immobilization strategy	Support material	Acronym	Reference
Encapsulation	Ca-alginate	POD-beads	Rezvani <i>et al.</i> <sup>20</sup>
Adsorption	Ca-alginate, H <sub>2</sub> O <sub>2</sub> and guaiacol K10-montmorillonite Ornamental rock powder	ModPOD-beads MK10-POD OR-POD	Coghetto <i>et al.</i> <sup>21</sup>
Magnetic nanozymes	Urea-NaOH	MN-POD	Sadaf <i>et al.</i> <sup>22</sup>

#### Adsorption on inorganic supports

The physical adsorption process was tested on two supports: K10-montmorillonite (Lot #STBH6207, Sigma-Aldrich, Merck, Brazil) and ornamental rock powder (donated from a local rock beneficiation process in Rio Grande do Sul, Brazil).

The ornamental rock is made up of acid volcanic rock rhyodacites from the *Província Paraná Fácies Caxias* formation (K1αcx), and it is composed of at least 50% of SiO<sub>2</sub> and several oxides. It arrived in the form of sludge (0.9% humidity) and went through an autoclave sterilization process (20 min, 1 atm, 120 °C), drying (2 h, 550 °C), and grinding before the immobilization process.

For both supports, the contact with enzymatic extract occurred under magnetic stirring in an ice bath for 10 min, following a methodology adapted from Coghetto *et al.*<sup>21</sup> Initially, 2 g of support was homogenized with 60 mL of sodium phosphate buffer (5 mmol L<sup>-1</sup> and pH 5.5). Then, the enzymatic extract was added at 3:10 v v<sup>-1</sup> enzyme:buffer ratio.

The suspension obtained from this procedure was vacuum-filtered to remove the liquid portion and kept in a desiccator for over 48 h for complete drying. The MK10-POD and OR-POD samples were obtained after grinding the content retained in the filtration procedure.

#### Magnetic nanozymes synthesis

The methodology for peroxidase incorporation onto magnetic Fe<sub>3</sub>O<sub>4</sub> nanoparticles by alkaline co-precipitation was adapted from Sadaf *et al.*<sup>22</sup> Initially, 2.4 mL of enzymatic extract was added to an alkaline solution containing 80 mL of distilled water, 12 g of urea, and 8 g of NaOH. The solution was stirred for 15 min at room temperature and then kept for 12 h in a refrigerator (4 °C). 100 mL of FeCl<sub>3</sub>/FeSO<sub>4</sub> solution (2:1 M ratio) was added to the prepared alkaline solution under continuous stirring at 60 °C.

The black precipitate obtained was first filtered, washed with distilled water, and subsequently with 95% ethanol to remove any non-reactive substances. The retained and washed film corresponded to the magnetic Fe<sub>3</sub>O<sub>4</sub> nanozymes (MN-POD), but additional steps were required to remove the moisture. Thus, the filter content was dried at 70 °C for 2 h, kept in a desiccator for 24 h, and milled.

#### Toxicological assessment of enzymatic treatment

The cytotoxicity and genotoxicity study of the dye solution, before and after the enzymatic treatment with free and immobilized peroxidase, was carried out with the organism *Allium cepa* according to the method described by Fiskesjö.<sup>23</sup>

Onion bulbs purchased in a local market were placed in water to germinate over 72 h, protected from direct sunlight. After root growth, they were exposed in duplicate to the treatments (pure or diluted in distilled water at a 1:8 ratio) for 48 h at room

temperature, maintaining a negative control exposed to tap water. The exposed roots were hydrolyzed in HCl at 1 mol L<sup>-1</sup> for 10 min at 60 °C, and the slides with the meristematic cells of *A. cepa* were prepared. This preparation is necessary for microscope analysis, and the cells were thus stained using the *Panótico Rápido*® kit (Laborclin).

Genotoxic effects were observed qualitatively using the Olympus CX21 Biological Microscope, in which changes, such as micronuclei, binucleate cells, and nuclear buds, were considered. The cytotoxic effects were quantified through mitotic changes, considering the different phases of cell division (metaphase, anaphase, and telophase). The mitotic index (MI) was calculated as the ratio between the number of cells observed in any of the division phases (NDC) and the total number of cells analyzed (NTC), according to Eqn (3), with a count of up to 100 cells per slide.

$$MI (\%) = \frac{NDC}{NTC} * 100 \quad (3)$$

#### Analytical procedures

Structural analyses of the support and immobilized peroxidase were performed by the Nuclear and Energy Research Institute (IPEN/CNEN-SP, Brazil), namely infrared spectrometry (FTIR) using Nicolet 6700 equipment (Thermo Scientific), and X-ray diffraction (XRD) using a Bruker D8 Advance 3 kW diffractometer equipped with a Cu-K alpha radiation tube and with a scintillation detector and reading samples at 2θ angles ranging from 20 to 90° in increments of 0.05°. Crystalline phases in the XRD analysis were identified by comparing the sample diffractogram with that of the International Centre for Diffraction Data (ICDD) using X'Pert High-Score Plus software.

Physical characterization (surface area and pore analyses) was performed by the Laboratory of Ceramics Processing (Department of Metallurgical and Materials Engineering, PMT-EPUSP, Brazil). Measurements were performed by N<sub>2</sub> adsorption using a Micromeritics Analyzer (Gemini III 2375 model). The Brunauer-Emmett-Teller (BET) multipoint method was applied to determine the specific surface area, and the Barrett-Joyner-Halenda (BJH) method to determine the pore volume and diameter (4 V/A). Before analysis, the samples were subjected to 24 h treatment under vacuum (100 mTorr) at 150 °C to ensure the removal of adsorbed species.

Using a silver chloride reference electrode, we quantified the oxidation potential of peroxidase according to Skoog *et al.*<sup>24</sup> ORP and pH measurements were performed using a pH/mV bench meter from HANNA Instruments HI2221. The values obtained were converted to mV vs. SHE, the standard unit of this electrochemical quantity.<sup>25</sup>

## Statistical analysis

The data from the tests underwent analysis of variance (ANOVA) using the software Statistica 8.0 and the online software Protimiza Experimental Design – <http://experimental-design.protimiza.com.br/>.<sup>26</sup>

## RESULTS AND DISCUSSION

### Relationship between enzymatic activity and discoloration potential

Preliminary tests with four synthetic dyes were carried out in the present work, aiming to find the affinity between *T. koningiopsis* peroxidase and the structure of the dyes, expecting enzymes to use the dye as a substrate in the enzymatic biooxidative reaction. Table 3 shows the results.

The greatest and most statistically significant discoloration occurred for the brown dye ( $54 \pm 1\%$ ) at a  $P$ -value  $<0.05$  by the Tukey test, when comparing the amount of enzymatic extract used (3833 or 7667 U) and the four types of dyes (Direct Red 9, Direct Blue 16, Direct Yellow 27, and Direct Brown 27). There was no statistical difference between the red and yellow dyes. The enzymatic treatment with 7667 U showed a statistically adequate color removal ( $22 \pm 2\%$ ) for the blue dye.

The different discoloration potentials observed between the dyes indicate the effects of structural diversity. Each dye has a specific molecular structure and molar weight (Table 1), which conveys the characteristics of color and dyeing. Considering the molecular aspect, the relationship between the structure and the enzymatic action depends on the type, number, and position (ortho or para) of the groups linked to the aromatic ring of the dyes. In this sense, the molecular aspect can accelerate, delay, or even cause complete inhibition of the enzymatic action.<sup>27</sup>

Due to its oxidative nature, there are several areas in which peroxidase could replace current techniques based on chemical catalysis.<sup>28</sup> Although different peroxidases have already been extensively studied, most studies use commercial, purified, and high-cost enzymes, making environmental applications unfeasible. The crude enzymatic extract showed specificity for Direct Brown 27 discoloration in this study. This result is promising since studies using peroxidases have reported their affinity with other dyes. For example, peroxidase extracted from industrial soybean residues efficiently degraded blue dye after 3 h of reaction (70% degradation).<sup>29</sup> Peroxidase from macrophytes performed well in the degradation of direct azo dyes, such as amaranth and black starch (93% and 87%, respectively, after 120 h of reaction).<sup>30</sup> Also, for the blue dye, two peroxidase sources (*Ipomea palmata* and *Saccharum spontaneum*) showed removals of 15% and 70%, respectively, after 1 to 2 h of treatment, indicating different specificities of plant peroxidase to the same dye.<sup>31</sup> Enzymatic

treatments conducted in other reactional systems also provided distinct color removal results, as shown by a previous study,<sup>18</sup> in which rice bran peroxidase removed 39% of the color after 3 h of reaction in a microwave system, while complete removal was achieved after 24 h in an orbital shaker.

In addition to the characteristics of the dyes, another possibility for different discoloration potentials is the enzymatic profile since we used a non-purified enzymatic extract. To investigate this hypothesis, we verified the effects of peroxidase and laccase activity on color removal results, using crude extracts from a previous study.<sup>14</sup> These extracts with different peroxidase and laccase profiles were applied to the brown dye discoloration process, and the results are presented in Fig. 1. In this experiment, the most remarkable discoloration ( $32 \pm 2\%$ ), which was statistically different from the other assays, occurred with enzymatic amounts of  $69 \pm 1$  U and  $0.02 \pm 0.01$  U of peroxidase and laccase, respectively (assay 5). These activities did not represent the highest enzymatic amount among the 15 assays performed. The maximum and most statistically relevant peroxidase amount was  $165 \pm 1$  U, in which the color removal was  $7 \pm 1\%$  (assay 8). For laccase, none of the assays reached activities above 0.02 U, and for this reason, its presence in the enzymatic extracts was considered irrelevant to the discoloration process.

The different peroxidase activity between the assays can be explained by the wide range of operating conditions in the fermentation process to produce the crude extract, such as temperature, pH, and agitation. Thus, the fermentation manipulation can provide an enzymatic profile with different performances in application processes, although the maximum activity did not represent the maximum discoloration potential.

Similar findings were observed when manganese peroxidase (MnP) and manganese independent (MIP) activities were evaluated.<sup>32</sup> The authors found a difference between the enzymatic activity and the discoloration of synthetic sulfonephthalein dyes. The variations in the discoloration reflect the differences in the isoenzyme composition of the MnP and MIP, resulting in a difference in the kinetic constants (varying the maximum rate of reaction from  $0.057$  to  $1$   $\text{U mL}^{-1}$ ) and the substrate specificity.<sup>32</sup>

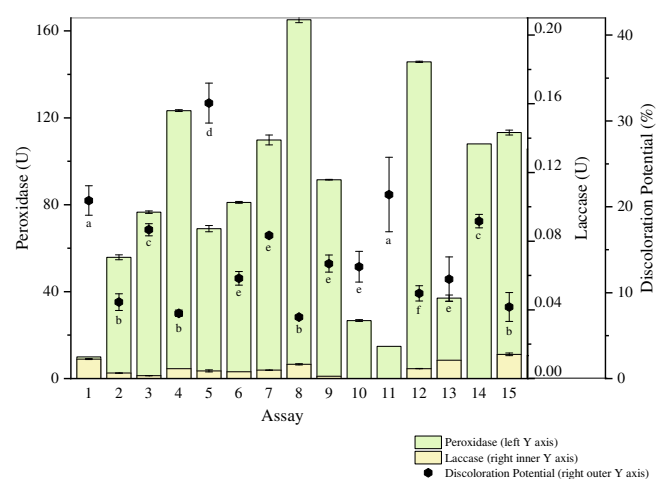


**Figure 1.** Relationship between the amount of peroxidase and laccase and the discoloration potential for brown dye. Note: The difference between enzyme production for the 15 assays is attributed to the variation in fermentation parameters: agitation (0–200 rpm), temperature (20–50 °C), and pH (3–14), following a Central Composite Rotatable Design.<sup>14</sup> Equal letters indicate that the discoloration potential results do not differ by the Tukey test at a 95% confidence level.

**Table 3.** Analysis of enzymatic treatment of synthetic dyes after 5 h of reaction

Enzymatic amount (U)	Discoloration potential (%)			
	Red dye	Blue dye	Yellow dye	Brown dye
3833	3 <sup>a</sup>	0 <sup>a</sup>	3 <sup>a</sup>	54 <sup>b</sup>
7667	3 <sup>a</sup>	22 <sup>c</sup>	4 <sup>a</sup>	46 <sup>d</sup>

Note: Means followed by equal letters indicate that the samples do not differ by the Tukey test at a 95% confidence level.

Another study also concluded that the reaction conducted with laccase alone did not degrade certain types of dyes. When the redox mediator violuric acid was added, however, the degradation efficiency reached 90% using 2/5 of the enzymatic activity of the tests without mediator.<sup>33</sup>

Thus, our results indicate that the change in operational parameters in fungal fermentation, in addition to providing enzymatic activity variations, must have influenced the composition of isoenzymes. It caused differences in specificity and interfered with the decolorization activity. It is noteworthy that, until this step of the work, no enzymatic manipulation method had been employed. Later, the reactions with immobilized peroxidase on different supports will be discussed.

### Catalytic properties of free and crude peroxidase

To insert a novel enzyme source into biotechnological processes, knowing and improving its catalytic properties and reactional conditions is essential. This work is the first to present the preliminary characterization of guaiacol peroxidase produced by *T. koningiopsis* in submerged fermentation supplemented exclusively by fresh microalgal biomass.

The extracellular enzymes of this fungus are rarely mentioned in the literature due to the difficulty in offering favorable conditions for fermentation and supplementation for its expression; this often involves costly processes for industrial applications.<sup>5</sup> Mäkelä *et al.*<sup>34</sup> report a wide variety of fungal peroxidases being applied as biocatalysts to reactions of environmental interest. In their study, the species *Trichoderma* is classified as Soft-Rot Fungi, about which little is known concerning peroxidase production. Azmi *et al.*<sup>35</sup> reported a combination of lignin peroxidase production in a more significant proportion and manganese peroxidase in a smaller proportion by *T. koningiopsis* when supplemented with oil palm fronds in solid-state fermentation.

Regardless of the peroxidase source, reaction thermodynamics influence enzymatic processes and need studies on varying pH, temperature, and availability of substrate and cosubstrate — all relevant factors in understanding the catalytic route.<sup>36</sup> These variables were investigated in the present work for the *T. koningiopsis* POD following a Plackett-Burman design. The results indicated enzyme stability even when subjected to adverse reaction conditions.

When subjected to pH ranging from 4.0–8.0 and temperatures from 20–80 °C, the enzymatic activity was not significantly affected at a 95% confidence level by the Tukey test. The enzyme:substrate and enzyme:cosubstrate ratios, conversely, negatively affected the enzymatic response with statistical relevance; that is, the POD activity was improved at the minimum levels studied (1 mL of POD for 0.5 mL of guaiacol and H<sub>2</sub>O<sub>2</sub>). None of the reaction conditions led to enzyme denaturation, maintaining a range from 5733 to 7700 U mg<sup>-1</sup>.

The peroxidase stability under varying conditions can be explained by the defense mechanisms previously developed by the fungus in its natural habitat.<sup>37</sup> Our microorganism was isolated from weeds already adapted to its ecosystem. The supplementation of the fermentation medium with microalgal biomass induced higher peroxidase productivity compared to synthetic supplementation,<sup>38</sup> confirming that stress induction during the fungus growth improves peroxidase production.

In contrast to the production behavior of other enzymes, stressful environments induce higher productivity of oxidoreductase enzymes and, consequently, fermentation conditions with less nutrient availability can result in greater peroxidase expression.

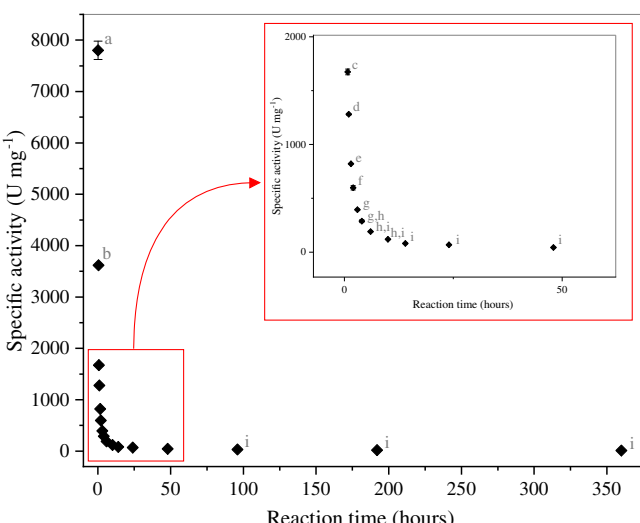


**Figure 2.** Enzymatic activity of *T. koningiopsis* over reaction time at pH 5.5 and 25 °C. Note: Equal letters indicate that the samples do not differ by the Tukey test at a 95% confidence level.

As the fungus fermentation process, the microalgae growth process occurred in a stressful environment, considering that it was cultivated with mainly ammonia and phosphorus availability.<sup>13</sup> Thus, according to a previous study,<sup>14</sup> there is synergism between fungi and microalgae, resulting in microalgae cells being incorporated into the fungal hyphae mesh. This synergy may have led to the obtention of an enzymatic extract with high resilience capacity in peroxidase activity, as shown in Fig. 2, where the interaction between the enzyme and reaction medium over time is demonstrated under constant environmental conditions.

To ensure that the evaporation or natural oxidation of the enzymatic extract did not induce false positives, controls were performed and considered in the enzymatic activity quantification. During the follow-up of the reaction, in the first 192 h, the pH and ORP values were maintained without statistically significant differences. The pH remained between  $7.3 \pm 0.1$  and  $7.6 \pm 0.1$ , and the ORP between  $195.6 \pm 3.3$  and  $214.2 \pm 1.1$  mV vs. SHE. The enzymatic activity varied from  $7801 \pm 179$  to  $11 \pm 2$  U mg<sup>-1</sup>, significantly decreasing and reaching its minimum value in 14 h.

In the last experimental point studied (360 h), the pH significantly dropped to  $6.5 \pm 0.4$ , and the redox potential increased to  $262.0 \pm 20.4$  mV vs. SHE. The standard error became high for this experimental point, and therefore, the experiment was stopped. In this sense, it is understood that after 360 h, it is unfeasible to maintain the enzymatic reaction without providing maintenance.

The constant decrease in enzymatic activity in the first hours of the reaction follows the same behavior observed in a published study for guaiacol peroxidase extracted from rice bran.<sup>39</sup> In 24 h of reaction, the observed activity had already fallen more than half of the initial value. In the present study, the fungus's intra and extracellular enzymatic systems can be critical in conducting the catalytic route through the quinone redox cycling mechanism. The presence of lignin and Fe<sup>2+</sup> in class II heme peroxidase structures induces a reaction that produces hydroxyl radicals in the presence of hydrogen peroxide. The enzymatic behavior shown in Fig. 2 can, thus, configure an advanced biooxidative process; in this process, the cosubstrate presence generates hydroxyl radicals, which in turn can regenerate cosubstrate. Therefore, the

enzymatic reaction is naturally maintained without the need for external interventions.<sup>40</sup>

The maintenance of positive ORP values during the reaction suggests that the reaction medium was receiving electrons, and that the substrate was oxidized. At the end of the reaction, the increase in ORP may have reflected the pH decrease since these parameters are inversely proportional.<sup>41</sup> The change in these parameters may have triggered the enzymatic reaction instability, which had already conducted multiple quinone redox cycles.

Considering the promising results of peroxidase activity and reaction maintenance even in adverse conditions, studies were conducted to monitor the enzymatic activity of the crude extract after storage. The results of this characterization are shown in Fig. 3.

The enzymatic extract activity (initially 7801 U mg<sup>-1</sup>) remained more stable at room temperature and in the refrigerator than in the freezer. For the storage condition between 18–28 °C, there was no significant difference in activity up to the 60th day, reaching 105 ± 3% of residual activity. However, between the 170th and the 400th day, activity decreased significantly from 80 ± 2% to zero. For storage at 4 °C, a considerable drop was observed up to 90 days (91 ± 1%), but on the 170th day, the RA returned to the initial value and then dropped to 7 ± 1% on the 400th day. The extract maintained at -10 °C initiated a significant and consistent drop of enzymatic activity after 15 days, reaching 63 ± 1% of RA in 90 days. From these results, we determined the kinetic constant  $k_d$  and the  $t_{1/2}$  of free *T. koningiopsis* POD: At 4 °C,  $k_d = 0.007 \text{ d}^{-1}$  and  $t_{1/2} = 103 \text{ d}$  ( $R^2 = 0.99$ ); at 18–28 °C,  $k_d = 0.002 \text{ d}^{-1}$  and  $t_{1/2} = 347 \text{ d}$  ( $R^2 = 0.97$ ).

It was possible to determine that the enzymatic extract can be kept in the refrigerator for up to 170 days without sudden drops in peroxidase activity. In addition, keeping the extract at room temperature proved to be an interesting option since the lower value of  $k_d$  and higher value of  $t_{1/2}$  indicated the greater stability of free-POD at this storage condition. The reasons for this activity behavior after storage will be discussed in the section 'Strategies for immobilizing *T. koningiopsis* peroxidase'.

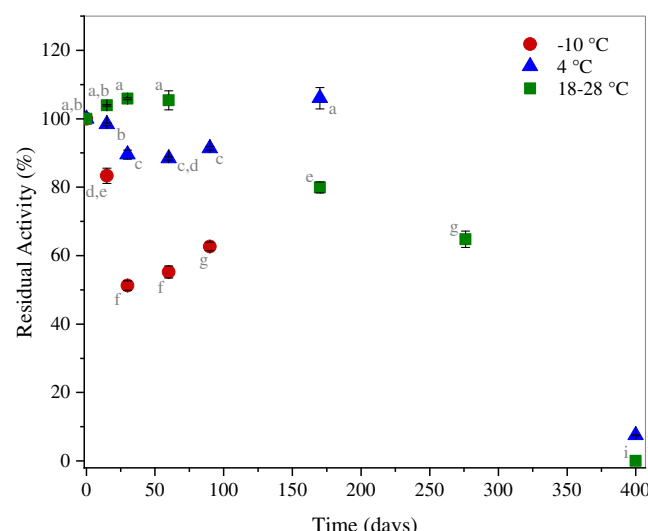


**Figure 3.** Monitoring free peroxidase activity stored at room temperature in the range 18–28 °C (■), refrigerator at 4 °C (▲), and freezer at -10 °C (●). Note: Equal letters indicate that the samples do not differ by the Tukey test at a 95% confidence level.

## Strategies for immobilizing *T. koningiopsis* peroxidase

Three different strategies were selected to conduct the immobilization process of the crude peroxidase extract (Free-POD) obtained in the fermentation process of *Trichoderma* supplemented by *Chlorella* spp. Two parameters were chosen to determine the immobilization efficiency: the residual activity and the discoloration potential of the brown dye solution at 100 mg L<sup>-1</sup>. This treatment process was selected because of its promising results in crude extract assays, the scarcity of studies on this dye, and the objective of inserting this bioproduct in the context of low-biodegradability contaminant remediation.

The immobilization strategies of this study were selected by considering the cost–benefit in the effluent treatment and circular economy scenario. The methods allowed for obtaining relevant results, with an increase in specific activity of up to 589% and color removal of up to 100%, as shown in Table 4.

RA values up to 100% indicate enzymatic retention in the support for the technique studied, and higher values demonstrate a positive interaction between support and enzyme. For the encapsulation method, it was possible to retain only 6% of the enzyme in the POD-beads, and 22% was lost to the calcium chloride solution. When the technique was modified (ModPOD-beads) by adding the POD substrate and cosubstrate to the beads to manipulate the affinity between enzyme and support, the retention was lower (3%), as was the activity in the solution (21%). These results indicate that the encapsulation technique is not suitable for *Trichoderma* peroxidase because of the low enzymatic retention in the beads. There was also a loss of enzymatic activity in the process since the RA balance considering beads and solution did not reach the reference value (100%).

Two different supports were studied in the adsorption method: the commercial clay MK10, which is widely used in enzymatic immobilization studies, and noncommercial ornamental rock powder (OR). The choice of this alternative support was motivated by the environmental problems related to the disposal of this waste material, which is constantly generated by rock processing industries. For both supports, enzymatic activity was lost to the buffer solution in which the contact process with peroxidase was conducted (19% for MK10 and 15% for OR). However, the commercial support had a greater affinity to the enzyme, with a 35% activity retention when compared to that of rock powder (11%). When making the RA balance, a loss of activity was observed in this case. However, compared to the encapsulation strategy, adsorption proved to be more promising and retained higher enzymatic activities in the supports.

Peroxidase from Horseradish (HRP)<sup>42</sup> and *Ganoderma lucidum*<sup>43</sup> were also encapsulated in Ca-alginate beads for dye degradation purposes. The authors added cross-linking agents (glutaraldehyde and syringaldehyde) during the immobilization procedure to improve efficiency.<sup>42,43</sup> The same strategy of adding mediators has been used to immobilize peroxidases by adsorption on clay carriers, resulting in improved efficiency.<sup>44–46</sup> Most immobilization studies use the strategy of previously purifying the enzyme, and then improving immobilization performance by adding such agents.<sup>5,47</sup> In the present study, the addition of glutaraldehyde during the encapsulation procedure resulted in a total loss of peroxidase activity (data not shown); therefore, it was considered an unfavorable strategy to be adopted for *Trichoderma* peroxidase.

The most advantageous process for maintaining and even increasing *Trichoderma* peroxidase activity after immobilization was magnetic nanozyme synthesis conducted with low-cost reagents. In this strategy, although part of the activity was lost

**Table 4.** Immobilization of *T. koningiopsis* POD and results of residual activity (RA), discoloration potential (DP) for brown dye, and physical characterization

Technique acronym	RA (%)	DP (%)	Physical analysis		
			BET specific surface area ( $\text{m}^2 \text{ g}^{-1}$ )	BJH pore volume ( $\text{cm}^3 \text{ g}^{-1}$ )	BJH pore diameter (nm)
Free-POD <sup>a</sup>	100	20	—	—	—
Control <sup>b</sup>	—	11	—	—	—
beads	—	43	—	—	—
POD-beads	6	36	—	—	—
ModPOD-beads	3	36	—	—	—
MK10	—	54	240.5	0.36	5.5
MK10-POD	35	8	228.6	0.30	5.1
OR	—	0	10.6	0.06	20.2
OR-POD	11	42	25.3	0.05	8.1
MN	—	56	86.7	0.09	4.0
MN-POD	689	100	53.9	0.16	10.4

Abbreviations: BET, Brunauer -Emmett -Teller method; BJH, Barrett-Joyner-Halenda method; DP, discoloration potential; MK10, K10-montmorillonite; MN, magnetic nanoparticles; OR, ornamental rock; POD, Peroxidase; RA, residual activity.

<sup>a</sup> Specific activity = 3066 U  $\text{mg}^{-1}$ .

<sup>b</sup> Dye solution (100 mg  $\text{L}^{-1}$ ) in the presence of 40 mg  $\text{L}^{-1}$  of hydrogen peroxide 35%.

to the solution in which the nanoparticles precipitated, the bond between POD and support favored the expression of catalytic activity. This process made it possible to obtain 21 111 U  $\text{mg}^{-1}$  of specific activity in MN-POD, representing a RA of 689% and relevant potential for application in biotechnological processes due to their magnetic properties.

As in the present study, commercial horseradish peroxidase was immobilized by magnetic nanocomposites by Chang *et al.*<sup>48</sup> exhibiting biochemical properties superior to those of the free enzyme, maintaining the RA at 100%, and improving resistance to temperature and pH variations. In turn, Monteiro *et al.*<sup>49</sup> investigated the immobilization of commercial *Candida antarctica* lipase onto magnetic nanoparticles and achieved RA values of up to 120% for a pH range between 8 and 10. This same RA value was achieved for POD magnetic nanozymes in a Sadaf *et al.*<sup>22</sup> study, but for a pH range between 3 and 4. Different methods are used for each nanoparticle synthesis study and each method results in particular biochemical characteristics. In addition, Zdarta *et al.*<sup>50</sup> highlight that the presence of many functional groups in the materials used for the synthesis gives the nanozymes a high surface area and porosity. These characteristics may justify the fixation of a large amount of enzyme in the nanoparticles and the increased catalytic activity compared to the free enzyme.

Among the techniques studied in the present work, MN-POD showed the most significant potential for discoloration, removing 100% of the color of the dye solution in 5 h. For treatments with POD immobilized by encapsulation and adsorption techniques, color removals of only up to 42% were obtained. The higher discoloration performance of MN-POD can be attributed to the presence of  $\text{Fe}^{2+}$  sites on the surface of nanozymes, inducing Fenton-like reactions between these sites and  $\text{H}_2\text{O}_2$ .<sup>51,52</sup> In short, the Fenton reaction initiates with the formation of a  $\text{Fe}^{2+}\text{-H}_2\text{O}_2$  complex and produces highly reactive oxygen species that promote the breakdown of organic compounds structure.<sup>53</sup>

From the data presented in Table 4, it is impossible to determine a direct relationship between enzymatic activity, discoloration potential, and the physical parameters of the enzyme carriers. For example, the surface area and pore size of magnetic  $\text{Fe}_3\text{O}_4$

nanoparticles (MN) were smaller than those of clay montmorillonite (MK10), but the nanoparticles retained more enzymes and had an improved result in the discoloration process. In addition, the discoloration results for the blank control did not result in conclusive contributions: taking MK10 and MK10-POD as an example, both have similar pore size and contact surface, but the support alone had a higher DP. In this sense, the results in Table 4 indicate that the enzymatic treatment depends on the cross-interaction between support, enzyme, and dye, giving complexity to the process that must be investigated in future works.

In addition to retaining enzymatic activity, the immobilization process must allow for reusing and storing the enzyme while maintaining catalytic efficiency. Accordingly, in addition to enzymatic retention, the immobilization process becomes relevant to provide a combined action between support and substrate that enhances the catalytic reaction, such as the induction of Fenton-like reactions above explained for the MN-POD tests. In this sense, a MN-POD sample with 283 256 U  $\text{mg}^{-1}$  was applied to the second batch brown dye treatment, in which 94% of discoloration was obtained maintaining the same conditions as the first batch.

The MN-POD sample was also subjected to 10 cycles of recovery and reinsertion in a reaction medium, as described in section 'Enzymatic activity quantification', to monitor the residual activity behavior. In cycles 2 and 3, a statistically significant decay in RA was observed, reaching the end of cycle 3 with  $37 \pm 10\%$ . From cycles 4 to 10, there was no considerable decay in RA. At the end of the experiment, the MN-POD had 13 546 U  $\text{mg}^{-1}$  of specific activity, corresponding to  $5 \pm 1\%$  of RA. Although the same amount of substrate was available in each cycle, the decay in activity and degradation efficiency is expected in reuse assays, considering that the enzyme's active sites and the support pore voids are filled over the cycles.<sup>9,54</sup>

In the storage test, MK10-POD, OR-POD, and MN-POD samples were stored at room temperature protected from direct sunlight, and their activity was measured after 2.5 months of the immobilization process. Compared to free-POD, the MK10-POD, OR-POD, and MN-POD remained with residual activities of 193%, 3%, and 10 637%, respectively, after the storage period. Additionally, MN-

POD activity was verified after about 8 and 18 months, and it had 9238% and 32% of RA, respectively.

Comparing with data in Table 4, the storage results reveal that only OR-POD lost enzymatic activity after storage, while MK10-POD and MN-POD gained it. For all samples, the specific activity of the immobilized enzyme remained higher than that in free form. The same behavior of activity increase after storage was observed for the crude extract. This phenomenon can be attributed to changes in the biochemical conformation of the protein or to an increase in the substrate specificity, which has already been reported in the literature for enzymes submitted to upstream processes, such as concentration and purification.<sup>8</sup>

The kinetic parameters  $k_d$  and  $t_{1/2}$  of *T. koningsiopsis* POD immobilized on magnetic nanoparticles at 18–28 °C are 0.006 d<sup>-1</sup> and 122 d ( $R^2 = 0.99$ ), respectively. The higher  $k_d$  and lower  $t_{1/2}$  of MN-POD, compared to those of free-POD at the same temperature, indicate that the immobilization process decreased the thermal stability; however, it is essential to note the superior specific activity of immobilized POD, even after 18 months, while the free enzyme lost its activity in 13 months.

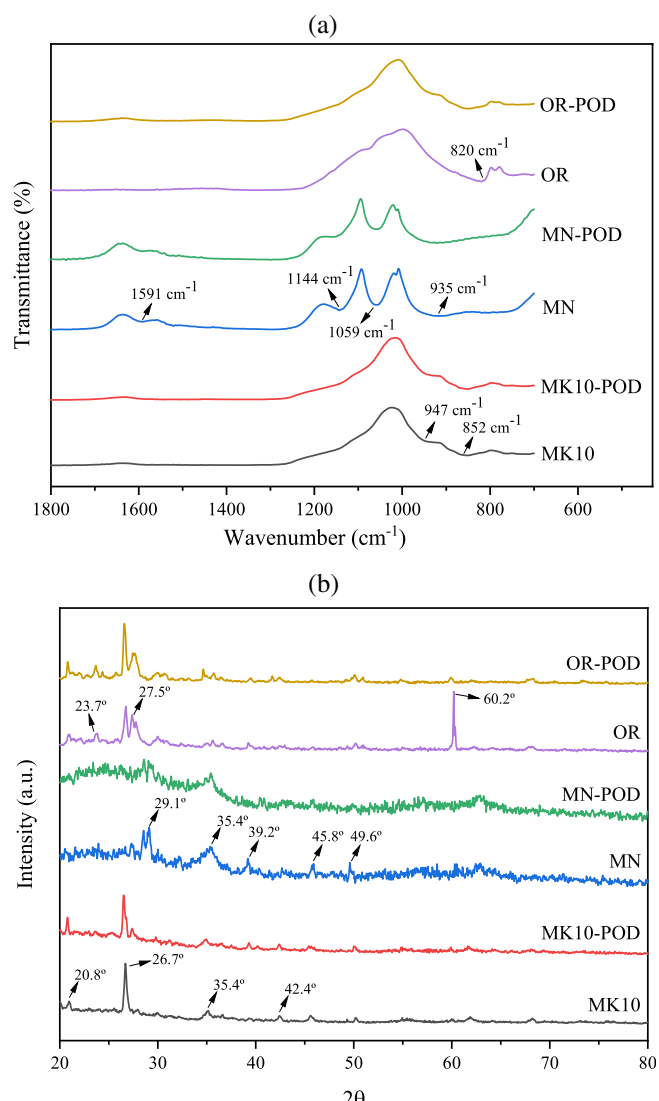


**Figure 4.** (a) FTIR and (b) XRD analyses of support and immobilized peroxidase.

This study made enzymatic activity improvements possible using simple immobilization techniques and considering cost-benefit, both of which are factors of great relevance in industrial applications. In addition, the bioproduct storage under mild conditions, the dispensation of chemical supplements, and the use of freeze-drying processes are advantages to its insertion for industrial applications in the enzyme market, which is in constant expansion according to the latest Global Industry Analysts report.<sup>4</sup>

#### Support and immobilized peroxidase characterization

OR-POD, MN-POD, and MK10-POD samples were submitted for characterization to understand the interactions between enzyme and support. In addition, support samples without enzymes were characterized.

The FTIR and XRD graphs are presented in Fig. 4 and, from a first examination, it is possible to observe the similarities when comparing the spectrum of the support to that of the support with enzyme; the transmittance peaks are in the same wavenumber range in FTIR analysis, and the intensity peaks appear in the same 2θ values in XRD patterns.

These findings indicate that the enzyme-support interaction did not modify the characteristic chemical bonds or the structural arrangement of the support material atoms during the immobilization processes. However, the enzyme-support interaction changed the surface area and pore size (Table 4). This aspect is positively relevant considering that immobilization aims to maintain both enzymatic and material properties. In the current work, this objective was achieved and the immobilization maintained peroxidase catalytic activity without affecting the chemical characteristics of the materials.

Another relevant observation regards the similarities between the two analyses of the peak behavior for the adsorption method (samples OR-POD, OR, MK10-POD, and MK10), indicating that ornamental rock powder is remarkably similar to the commercial clay MK10. The FTIR spectra of these samples show weak peaks between 820 and 947 cm<sup>-1</sup> (Fig. 4(a)), corresponding to Al – Al – OH, Al – Fe – OH and Al – Mg – OH deformation, and Si – O stretching mode. The absence of peaks around 1000 cm<sup>-1</sup> indicates no water content in the samples.<sup>55</sup> The inferior OR capacity to adsorb the enzyme can be attributed to its lower surface area (10.6 m<sup>2</sup> g<sup>-1</sup>) compared to MK10 (240.5 m<sup>2</sup> g<sup>-1</sup>).

For MN and MN-POD samples, small intensity peaks were observed at 935, 1059, and 1144 cm<sup>-1</sup>, suggesting the presence of a significant amount of specifically adsorbed sulfate groups. These can occupy external and internal surfaces (sulfated goethite), and the amount of these groups is related to the acidic pH. The peak at 1591 cm<sup>-1</sup> indicates H<sub>2</sub>O bending vibrations.<sup>56</sup>

In XRD analysis of magnetic nanoparticles, the peaks indicated in Fig. 4(b), between 27 and 50°, confirm goethite presence as a single phase, which is characteristic of superparamagnetic particles.<sup>57</sup> Also, characteristic peaks corresponding to planes of Fe<sub>3</sub>O<sub>4</sub> and MgO crystals were observed, whose low intensity is due to the small size of the synthesized particles.<sup>58</sup>

The amorphous characteristic of the MN and MN-POD samples is another positive finding from the XRD analysis. It is beneficial for many applications due to its superior catalytic activity and superparamagnetic behavior compared with crystalline structures.<sup>59</sup> Experimental conditions are relevant in amorphous Fe<sub>3</sub>O<sub>4</sub> synthesis, especially regarding particle size and structure homogeneity.<sup>60</sup> In this sense, the method we used can be considered suitable for obtaining excellent magnetic nanozymes with increased pore volume and diameter (0.16 cm<sup>3</sup> g<sup>-1</sup> and 10.4 nm,

**Table 5.** Disorders in cell division of *A. cepa* after being exposed for 48 h to enzymatically treated dye solutions

Treatment assay	Solution parameters		
	DP (%)	pH	MI (%)
Negative control <sup>a</sup>	–	~7.0	18
Crude dye solution	0	8.3	19
Free-POD	20	7.6	8 and 7 <sup>b</sup>
ModPOD-beads	36	5.9	65 and 22 <sup>b</sup>
MK10-POD	8	7.5	29 and 10 <sup>b</sup>
OR-POD	42	7.6	7 <sup>b</sup>
MN-POD	100	2.4	89 and 3 <sup>b</sup>

<sup>a</sup> Tap water.<sup>b</sup> Enzymatically treated dye solution diluted at 1:8.

respectively) compared to magnetic nanoparticles without enzyme (MN sample, Table 4).

From the XRD patterns in Fig. 4(b), it is possible to verify similar crystalline structures of OR-POD, OR, MK10-POD, and MK10. The

$2\theta$  values variation between samples does not exceed  $0.5^\circ$ , but there are some differences in intensity. The main highlight is the occurrence of an intense peak at  $60.2^\circ$  for OR, confirming that this material has  $\text{SiO}_2$ , as expected, since it is the primary mineral of this material. Small intense peaks associated with  $\text{SiO}_2$  are also clearly observed at  $26.7$  and  $27.5^\circ$  for OR and MK10, respectively. The remaining low intense peaks in Fig. 4(b) are natural mineral signatures expected for these materials.<sup>55</sup>

#### Toxicological assessment of enzymatic treatments

The test organism selected was *A. cepa*, in which disorders in cell division can be counted and compared using the mitotic index. With a negative control as a standard (cells exposed to tap water), higher or lower mitotic index (MI) values indicate disorders in the mitosis process, as shown in Table 5.

According to Fiskejö,<sup>23</sup> one of the precursors of this test, the meristematic onion cells study is indicated for environmental monitoring, presenting advantages such as low cost, easy execution, and possibilities of microscopic research, along with the possibility to evaluate the chromosomal damage caused by an aqueous matrix and disorders in cell division.

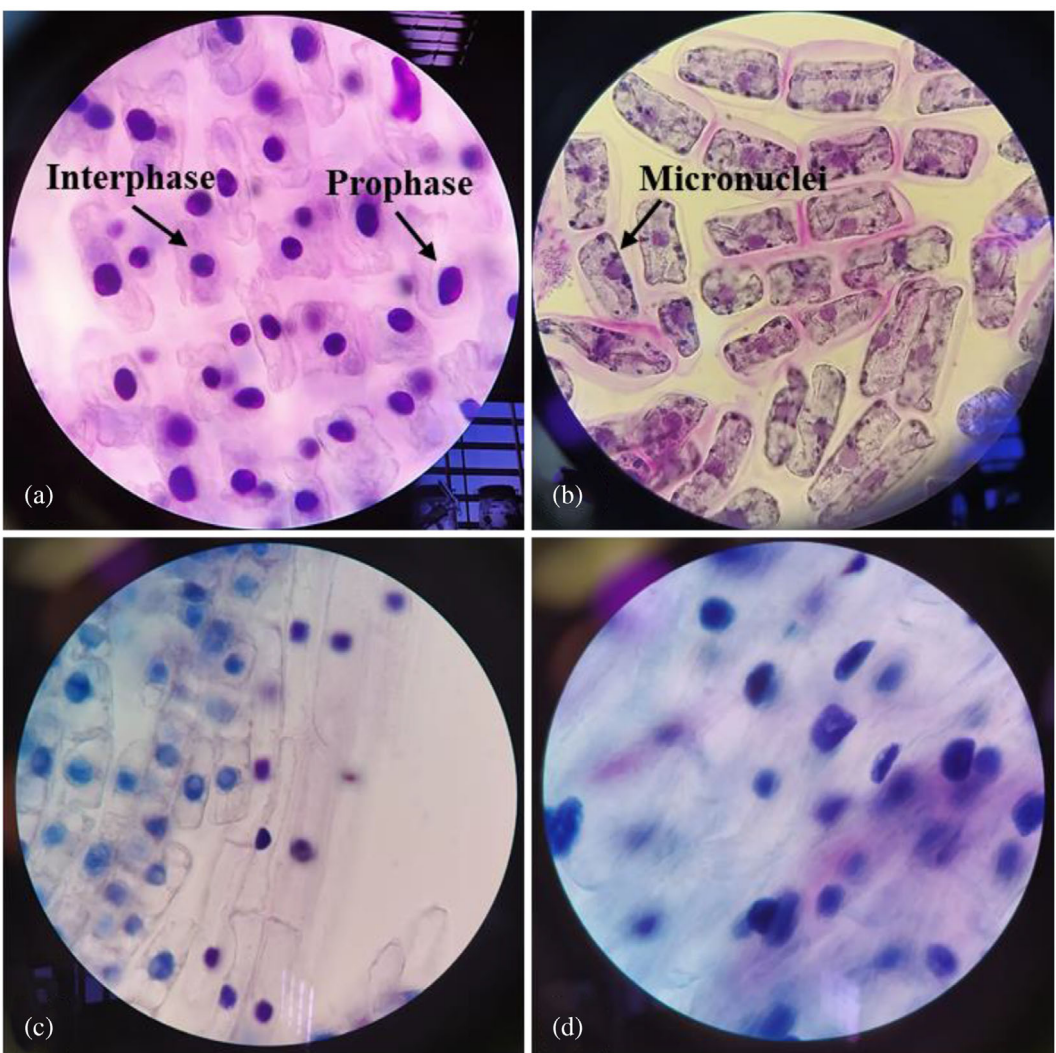


**Figure 5.** Microscopic observations in *A. cepa* cells, with 100 $\times$  magnification lens, for (a) tap water, (b) free-POD at 1:8 dilution, (c) MN-POD, and (d) MN-POD at 1:8 dilution.

Qualitative observations on slides made it possible to detect chromosomal aberrations caused by enzymatic treatments. In Fig. 5, these damages are indicated to emphasize them in some of the treatments. The presence of micronuclei in free-POD treatment is one of the main genotoxic highlights, indicating that the crude enzymatic extract can induce uncontrolled cell division and, possibly, tumor formation.<sup>61</sup> In contrast, chromosomal aberrations were not observed for the other treatments, indicating that enzymatic immobilization is relevant to eliminating genotoxic effects. However, disorders in the mitosis process were quantified for all assays, as shown in Table 5.

In the MN-POD assay, for which complete discoloration was achieved, the phenomenon of cell division acceleration was quantified, increasing by five times compared to the negative control. When the sample was diluted at 1:8, a delay in cell division occurred (0.2 times); it was possible to verify this by MI values (Table 5) and visual comparison between images (a), (c), and (d) of Fig. 5. As in the negative control (tap water), the cells were predominantly in the prophase phase for the samples enzymatically treated, i.e., the first stage of cell division. In turn, all the division phases were visualized in the dye solution before treatment, although the MI value was only 1.1 times higher than that of the negative control.

The findings regarding the cell division phases are relevant since cells in metaphase and anaphase are more susceptible to chromosomal changes and DNA abnormalities.<sup>62</sup> In this sense, cytotoxic and genotoxic analyses provide complementary results since mitotic indexes close to the negative control value do not guarantee the absence of chromosomal aberrations. According to Fiskesjö,<sup>23</sup> toxicological assessment can diagnose possible behaviors of the test organism when exposed to treatments, but it is a result of multiple combined factors. For example, the author found a relationship between the pH of the solution and toxicological effects; however, it was not possible to find this direct relationship between disorder in cell division and pH in our work.

Miranda-Mandujano *et al.*<sup>29</sup> and Feng *et al.*<sup>63</sup> attributed the increase in toxic effects after enzymatic reaction to the formation of transformation products during the catalytic route. It is believed that, in our study, these products with distinct harmful effects may have been formed after enzymatic treatment because of the disorders caused by cell division. These disorders may be related to the different enzymatic conformations obtained by the immobilization strategies, considering that different cytotoxic behaviors occurred between tests, even with equal dye concentrations and operating conditions.

The samples' dilution before exposure to *A. cepa* cells changed cell division behavior, as indicated in Table 5. It is understood that the search for a dilution factor in the context of the treatment proposed in this work can be one of the strategies for reaching MI values closer to that of the negative control. It is worth mentioning that the degradation of different compounds by the enzymatic route presents different responses from the toxicological point of view. Therefore, it is relevant that treatments inserted in other contexts are carefully analyzed and closely consider multiple aspects.

## CONCLUSIONS

The search for solutions to problems caused by human activities has become increasingly necessary. This work discusses proposals for producing and immobilizing peroxidase using low-cost processes and reagents and providing a bioproduct

with oxidative potential for pollutant remediation in aqueous matrices.

The enzymatic extract was produced by submerged fermentation of the fungus *T. koningiopsis*, supplemented exclusively by microalgae cultivated in swine wastewater digestate; this production easily places it in the circular economy context. The extract showed potential for insertion in advanced biooxidative reactions due to the presence of guaiacol peroxidase with good stability when subjected to extreme reaction conditions. The bioproduct presented an adequate behavior, expressing specific activity of up to 7801 U mg<sup>-1</sup> in the free form and 21 111 U mg<sup>-1</sup> when immobilized. It is worth highlighting the promising results in storage tests at room temperature for up to 18 months, maintaining the catalytic efficiency over time.

The *T. koningiopsis* peroxidase and the immobilization processes studied in the present work were also promising considering its potential for synthetic dye discoloration, achieving removal of 100% of the color in 5 h, and of 94% in the enzyme reuse test, even with a drop in the specific activity. The technique of magnetic nanzyme synthesis proved to be the most promising from the point of view of both discoloration potential and the maintenance of residual activity. Nanzymes also have the advantage of direct recovery with the aid of a magnetic field, enabling reuse for multiple catalytic cycles. Free-POD showed cytotoxic and genotoxic effects in assays with the test organism *A. cepa*, while immobilized POD did not show genotoxicity.

## STATEMENTS AND DECLARATIONS

### COMPETING INTERESTS

The authors declare that they have no conflict of interest.

### ETHICS APPROVAL AND CONSENT TO PARTICIPATE

Not applicable.

### CONSENT FOR PUBLICATION

All authors agreed with this publication.

### AVAILABILITY OF DATA AND MATERIALS

The datasets generated for this study are available on request to the corresponding author.

### AUTHORS' CONTRIBUTIONS

N Klanovicz: Conceptualization, investigation, data curation, formal analysis, writing – original draft. FS Stefanski: Conceptualization, investigation, data curation, formal analysis, writing – original draft. AF Camargo: Conceptualization, investigation, data curation, formal analysis.

W Michelon: Conceptualization, investigation, data curation, formal analysis. H Treichel: Supervision, project administration, funding acquisition, writing – review & editing. ACSC Teixeira: Supervision, project administration, funding acquisition, writing – review & editing.

## ACKNOWLEDGEMENTS

The authors are grateful to the following Brazilian research agencies: Fundação de Amparo à Pesquisa do Estado do Rio Grande do Sul – FAPERGS, Coordenação de Aperfeiçoamento de Pessoal de Nível Superior – Brasil (CAPES), and Conselho Nacional de Desenvolvimento Científico e Tecnológico – CNPq (grant #311230-2020-2); to the research group at Laboratório de Experimentação e Análises Ambientais (Embrapa Suínos e Aves – Concórdia, Brazil); to Dr. Solange Sakata from Centro de Tecnologia das Radiações (Instituto de Pesquisas Energéticas e Nucleares – São Paulo, Brazil); and to Dr. Bruno Ramos from the Laboratory of Ceramics Processing (Department of Metallurgical and Materials Engineering, Escola Politécnica, Universidade de São Paulo – São Paulo, Brazil).

## REFERENCES

- Ali L, Algaithi R, Habib HM, Souka U, Rauf MA and Ashraf S, Soybean peroxidase-mediated degradation of an azo dye - a detailed mechanistic study. *BMC Biochem* **14**:35 (2013). <https://doi.org/10.1186/1471-2091-14-35>.
- Singh MP, Vishwakarma SK and Srivastava AK, Bioremediation of direct blue 14 and extracellular Ligninolytic enzyme production by white rot fungi: *Pleurotus* spp. *Biomed Res Int* **2013**:180156 (2013). <https://doi.org/10.1155/2013/180156>.
- Saroi S, Kumar K, Pareek N, Prasad R and Singh RP, Biodegradation of azo dyes acid red 183, direct blue 15 and direct red 75 by the isolate *Penicillium oxalicum* SAR-3. *Chemosphere* **107**:240–248 (2014). <https://doi.org/10.1016/j.chemosphere.2013.12.049>.
- Research and Markets, *Industrial Enzymes—Global Market Trajectory & Analytics, Report ID 338655*. Global Industry Analysts, Dublin, Ireland, p. 402 (2021).
- Jun LY, Yon LS, Mubarak NM, Bing CH, Pan S, Danquah MK et al., An overview of immobilized enzyme technologies for dye and phenolic removal from wastewater. *J Environ Chem Eng* **7**:102961 (2019). <https://doi.org/10.1016/j.jece.2019.102961>.
- Morsi R, Bilal M, Iqbal HMN and Ashraf SS, Laccases and peroxidases: the smart, greener and futuristic biocatalytic tools to mitigate recalcitrant emerging pollutants. *Sci Total Environ* **714**:136572 (2020). <https://doi.org/10.1016/j.scitotenv.2020.136572>.
- Viancelli A, Michelon W, Rogovski P, Cadamuro RD, de Souza EB, Fongaro G et al., A review on alternative bioprocesses for removal of emerging contaminants. *Bioprocess Biosyst Eng* **43**:2117–2129 (2020). <https://doi.org/10.1007/s00449-020-02410-9>.
- Abedi D, Zhang L, Pyne M, Chou CP, *Enzyme Biocatalysis, in Comprehensive Biotechnology*, Moo-Young M. Elsevier, Canada, pp. 15–24 (2011). <https://doi.org/10.1016/B978-0-444-64046-8.00003-3>.
- Shakerian F, Zhao J and Li S-P, Recent development in the application of immobilized oxidative enzymes for bioremediation of hazardous micropollutants—a review. *Chemosphere* **239**:124716 (2020). <https://doi.org/10.1016/j.chemosphere.2019.124716>.
- Bilal M, Rasheed T, Zhao Y, Iqbal HMN and Cui J, "smart" chemistry and its application in peroxidase immobilization using different support materials. *Int J Biol Macromol* **119**:278–290 (2018). <https://doi.org/10.1016/j.ijbiomac.2018.07.134>.
- Anawar HM and Ahmed G, Combined electrochemical-advanced oxidation and enzymatic process for treatment of wastewater containing emerging organic contaminants, in *Emerging and Nanomaterial Contaminants in Wastewater*, ed. by Mishra AK, Anawar HM and Drouiche N. Elsevier, Amsterdam, pp. 277–307 (2019). <https://doi.org/10.1016/B978-0-12-814673-6.00010-3>.
- Reichert Júnior FW, Scariot MA, Forte CT, Pandolfi L, Dil JM, Weirich S et al., New perspectives for weeds control using autochthonous fungi with selective bioherbicidal potential. *Helicon* **5**:e01676 (2019). <https://doi.org/10.1016/j.helicon.2019.e01676>.
- Michelon W, Da Silva MLB, Mezzari MP, Pirolli M, Prandini JM and Soares HM, Effects of nitrogen and phosphorus on biochemical composition of microalgae polyculture harvested from Phycoremediation of piggyback wastewater Digestate. *Appl Biochem Biotechnol* **178**:1407–1419 (2016). <https://doi.org/10.1007/s12010-015-1955-x>.
- Stefanski FS, Camargo AF, Scapini T, Bonatto C, Venturini B, Weirich SN et al., Potential use of biological herbicides in a circular economy context: a sustainable approach. *Front Sustainable Food Syst* **4**:521102 (2020). <https://doi.org/10.3389/fsufs.2020.521102>.
- Garda-Buffon J, Kupski L and Badiola-Furlong E, Deoxynivalenol (DON) degradation and peroxidase enzyme activity in submerged fermentation. *Food Sci Technol* **31**:198–203 (2011). <https://doi.org/10.1590/S0101-20612011000100030>.
- Hou H, Zhou J, Wang J, Du C and Yan B, Enhancement of laccase production by *Pleurotus ostreatus* and its use for the decolorization of anthraquinone dye. *Process Biochem* **39**:1415–1149 (2004). [https://doi.org/10.1016/S0032-9592\(03\)00267-X](https://doi.org/10.1016/S0032-9592(03)00267-X).
- Bradford M, A rapid and sensitive method for the quantitation of microgram quantities of protein utilizing the principle of protein-dye binding. *Anal Biochem* **72**:248–254 (1976). <https://doi.org/10.1006/abio.1976.9999>.
- Klanovicz N, Camargo AF, Stefanski FS, Zanivan J, Scapini T, Pollon R et al., Advanced oxidation processes applied for color removal of textile effluent using a home-made peroxidase from rice bran. *Bioprocess Biosyst Eng* **43**:261–272 (2020). <https://doi.org/10.1007/s00449-019-02222-6>.
- Feltrin A, Garcia S, Caldas S, Primel E, Badiola-Furlong E and Garda-Buffon J, Characterization and application of the enzyme peroxidase to the degradation of the mycotoxin DON. *J Environ Sci Health, Part B* **52**:777–783 (2017). <https://doi.org/10.1080/03601234.2017>.
- Rezvani F, Azargosha H, Jamialahmadi O, Hashemi-Najafabadi S, Mousavi SM and Shojaosadati SA, Experimental study and CFD simulation of phenol removal by immobilization of soybean seed coat in a packed-bed bioreactor. *Biochem Eng J* **101**:32–43 (2015). <https://doi.org/10.1016/j.bej.2015.04.019>.
- Coghetto CC, Scherer RP, Silva MF, Golunski S, Pergher SBC, de Oliveira D et al., Natural montmorillonite as support for the immobilization of inulinase from *Kluyveromyces marxianus* NRRL Y-7571. *Bio-catal Agric Biotechnol* **1**:284–289 (2012). <https://doi.org/10.1016/j.bcab.2012.06.005>.
- Sadaf A, Ahmad R, Ghorbal A, Elfalleh W and Khare SK, Synthesis of cost-effective magnetic nano-biocomposites mimicking peroxidase activity for remediation of dyes. *Environ Sci Pollut Res* **27**:27211–22720 (2020). <https://doi.org/10.1007/s11356-019-05270-3>.
- Fiskesjö G, The *allium* test as a standard in environmental monitoring. *Hereditas* **102**:99–112 (1985). <https://doi.org/10.1111/j.1601-5223.1985.tb00471.x>.
- Skoog DA, West DM, Holler J and Crouch SR, *Fundamentals of Analytical Chemistry*. Cengage Learning, Boston, p. 1072 (2013).
- Brown TE, LeMay HE, Bursten BE, Murphy C and Woodward P, *Chemistry: The Central Science in SI Units*. Pearson, London, p. 1248 (2017).
- Rodrigues MI and lemma AF, *Experimental Design and Process Optimization*. CRC Press, Florida, p. 336 (2014).
- Dawkar VV, Jadhav UU, Telke AA and Govindwar SP, Peroxidase from *bacillus* sp. VUS and its role in the decolorization of textile dyes. *Bio-technol. Bioprocess Eng* **14**:361–368 (2009). <https://doi.org/10.1007/s12257-008-0242-x>.
- Hamid M and Khalil-ur-Rehman, Potential applications of peroxidases. *Food Chem* **115**:1177–1186 (2009). <https://doi.org/10.1016/j.foodchem.2009.02.035>.
- Miranda-Mandujano E, Moeller-Chávez G, Villegas-Rosas O, Buitrón G and Garzón-Zúñiga M, Decolourization of direct blue 2 by peroxidases obtained from an industrial soybean waste. *Water SA* **44**:204–210 (2018). <https://doi.org/10.4314/wsa.v44i2.06>.
- Haddaji D, Bousselmi L, Saadani O, Nouairi I and Ghrabi-Gammar Z, Enzymatic degradation of azo dyes using three macrophyte species: *Arundo donax*, *Typha angustifolia* and *Phragmites australis*. *Desalin Water Treat* **1129**:1138 (2014). <https://doi.org/10.1080/19443994.2014.884475>.
- Shaffiq TS, Roy JJ, Nair RA and Abraham TE, Degradation of textile dyes mediated by plant peroxidases. *Appl Biochem Biotechnol* **102-103**:315–326 (2002). <https://doi.org/10.1385/ABAB:102-103:1-6:315>.
- Shrivastava R, Christian V and Vyas BRM, Enzymatic decolorization of sulfonphthalein dyes. *Enzyme Microb Technol* **36**:333–337 (2005). <https://doi.org/10.1016/j.enzmictec.2004.09.004>.
- Soares GMB, Pessoa de Amorim MT and Costa-Ferreira M, Use of laccase together with redox mediators to decolorize Remazol brilliant blue R. *J Biotechnol* **89**:123–129 (2001). [https://doi.org/10.1016/S0168-1656\(01\)00302-9](https://doi.org/10.1016/S0168-1656(01)00302-9).
- Mäkelä MR, Hildén KS and Kuuskeri J, Fungal lignin-modifying peroxidases and H<sub>2</sub>O<sub>2</sub>-producing enzymes, in *Reference Module in Life Sciences*, ed. by Zaragoza O and Casadevall A. Elsevier, Amsterdam, pp. 1–10 (2014).

247–259 (2020). <https://doi.org/10.1016/B978-0-12-809633-8.21127-8>.

35 Azmi MA, Yusof MT, Zunita Z and Hassim HA, Enhancing the utilization of oil palm fronds as livestock feed using biological pre-treatment method. *IOP Conf Ser Earth Environ Sci* **230**:012077 (2019). <https://doi.org/10.1088/1755-1315/230/1/012077>.

36 Nelson DL and Cox MM, *Lehninger Principles of Biochemistry*. W H Freeman, New York, p. 1340 (2012).

37 Baiyee B, Ito S and Sunpapao A, *Trichoderma asperellum* T1 mediated antifungal activity and induced defense response against leaf spot fungi in lettuce (*Lactuca sativa* L.). *Physiol Mol Plant Pathol* **106**:96–101 (2019). <https://doi.org/10.1016/j.pmpp.2018.12.009>.

38 Bordin ER, Frumí Camargo A, Rossetto V, Scapini T, Modkovski TA, Weirich S *et al.*, Non-toxic bioherbicides obtained from *Trichoderma koningiopsis* can be applied to the control of weeds in agriculture crops. *Ind Biotechnol* **14**:157–163 (2018). <https://doi.org/10.1089/ind.2018.0007>.

39 Klanovicz N, Warken A, Paliga L, Camargo AF, Scapini T, Buffon JG *et al.*, One-step procedure for peroxidase concentration, dye separation, and color removal by aqueous two-phase system. *Environ Sci Pollut Res* **28**:9097–9106 (2021). <https://doi.org/10.1007/s11356-020-11412-9>.

40 Vasilidiou IA, Molina R, Pariente MI, Christoforidis KC, Martinez F and Melero JA, Understanding the role of mediators in the efficiency of advanced oxidation processes using white-rot fungi. *Chem Eng J* **359**:1427–1435 (2019). <https://doi.org/10.1016/j.cej.2018.11.035>.

41 Battistuzzi G, Bellei M, Bortolotti CA and Sola M, Redox properties of heme peroxidases. *Arch Biochem Biophys* **500**:21–36 (2010). <https://doi.org/10.1016/j.abb.2010.03.002>.

42 Liu X, Xue P, Jia F, Shi K, Gu Y, Ma L *et al.*, A novel approach to efficient degradation of indole using co-immobilized horseradish peroxidase-syringaldehyde as biocatalyst. *Chemosphere* **262**:128411 (2021). <https://doi.org/10.1016/j.chemosphere.2020.128411>.

43 Bilal M and Asgher M, Dye decolorization and detoxification potential of Ca-alginate beads immobilized manganese peroxidase. *BMC Biotechnol* **15**:111 (2015). <https://doi.org/10.1186/s12896-015-0227-8>.

44 Kim HJ, Suma Y, Lee SH, Kim J-A and Kim HS, Immobilization of horseradish peroxidase onto clay minerals using soil organic matter for phenol removal. *J Mol Catal B: Enzym* **83**:8–15 (2012). <https://doi.org/10.1016/j.molcatb.2012.06.012>.

45 Zhou F, Luo J, Qi B, Chen X and Wan Y, Horseradish peroxidase immobilized on multifunctional hybrid microspheres for aflatoxin B1 removal: will enzymatic reaction be enhanced by adsorption? *Ind Eng Chem Res* **58**:11710–11719 (2019). <https://doi.org/10.1021/acs.iecr.9b02094>.

46 Pavlovic M, Rouster P, Somosi Z and Szilagyi I, Horseradish peroxidase-nanoclay hybrid particles of high functional and colloidal stability. *J Colloid Interface Sci* **524**:114–121 (2018). <https://doi.org/10.1016/j.jcis.2018.04.007>.

47 Khalid N, Kalsoom U, Ahsan Z and Bilal M, Non-magnetic and magnetically responsive support materials immobilized peroxidases for biocatalytic degradation of emerging dye pollutants—a review. *Int J Biol Macromol* **207**:387–401 (2022). <https://doi.org/10.1016/j.ijbiomac.2022.03.035>.

48 Chang Q, Jiang G, Tang H, Li N, Huang J and Wu L, Enzymatic removal of chlorophenols using horseradish peroxidase immobilized on superparamagnetic  $\text{Fe}_3\text{O}_4$ /graphene oxide nanocomposite. *Chin J Catal* **36**:961–968 (2015). [https://doi.org/10.1016/S1872-2067\(15\)60856-7](https://doi.org/10.1016/S1872-2067(15)60856-7).

49 Monteiro RRC, Lima PJM, Pinheiro BB, Freire TM, Dutra LMU, Fechine PBA *et al.*, Immobilization of lipase a from *Candida Antarctica* onto chitosan-coated magnetic nanoparticles. *Int J Mol Sci* **20**: 4018 (2019). <https://doi.org/10.3390/ijms20164018>.

50 Zdarta J, Meyer AS, Jesionowski T and Pinelo M, Developments in support materials for immobilization of oxidoreductases: a comprehensive review. *Adv Colloid Interface Sci* **258**:1–20 (2018). <https://doi.org/10.1016/j.cis.2018.07.004>.

51 Wang N, Zhu L, Wang D, Wang M, Lin Z and Tang H, Sono-assisted preparation of highly-efficient peroxidase-like  $\text{Fe}_3\text{O}_4$  magnetic nanoparticles for catalytic removal of organic pollutants with  $\text{H}_2\text{O}_2$ . *Ultrason Sonochem* **17**:526–533 (2010). <https://doi.org/10.1016/j.ultsonch.2009.11.001>.

52 Ballesteros CAS, Mercante LA, Alvarenga AD, Facure MHM, Schneider R and Correa DS, Recent trends in nanozymes design: from materials and structures to environmental applications. *Mater Chem Front* **5**: 7419–7451 (2021). <https://doi.org/10.1039/D1QM00947H>.

53 Kanakaraju D, Glass BD and Oelgemöller M, Advanced oxidation process-mediated removal of pharmaceuticals from water: a review. *J Environ Manage* **219**:189–207 (2018). <https://doi.org/10.1016/j.jenvman.2018.04.103>.

54 Sastre DE, Reis EA and Marques Netto CGC, Strategies to rationalize enzyme immobilization procedures, in *Methods in Enzymology*, ed. by Kumar CV. Elsevier, Amsterdam, pp. 81–110 (2020). <https://doi.org/10.1016/bs.mie.2019.09.003>.

55 Ahmed A, Chaker Y, Belarbi EH, Abbas O, Chotard JN, Abassi HB *et al.*, XRD and ATR/FTIR investigations of various montmorillonite clays modified by monocationic and dicationic imidazolium ionic liquids. *J Mol Struct* **1173**:653–664 (2018). <https://doi.org/10.1016/j.molstruc.2018.07.039>.

56 Gotić M and Musić SM, FT-IR and FE SEM investigation of iron oxides precipitated from  $\text{FeSO}_4$  solutions. *J Mol Struct* **834–836**:445–453 (2007). <https://doi.org/10.1016/j.jmolstruc.2006.10.059>.

57 Gotić M, Musić S, Popović S and Sekovanić L, Investigation of factors influencing the precipitation of iron oxides from Fe(II) containing solutions. *Croat Chem Acta* **81**:569–578 (2008).

58 Beyki MH, Bayat M and Shemirani F, Fabrication of core-shell structured magnetic nanocellulose base polymeric ionic liquid for effective biosorption of Congo red dye. *Bioresour Technol* **218**:236–234 (2016). <https://doi.org/10.1016/j.biortech.2016.06.069>.

59 Machala L, Zboril R and Gedanken A, Amorphous iron(III) oxide - a review. *J Phys Chem B* **111**:4003–4018 (2007). <https://doi.org/10.1021/jp064992s>.

60 Jolivet JP, Tronc E and Vayssières L, Formation of magnetic spinel iron oxide in solution, in *Nanophase Materials*, ed. by Hadjipanayis GC and Siegel RW. Springer, Netherlands, pp. 45–48 (1994). [https://doi.org/10.1007/978-94-011-1076-1\\_5](https://doi.org/10.1007/978-94-011-1076-1_5).

61 Fernandes TCC, Mazzeo DEC and Marin-Morales MA, Mechanism of micronuclei formation in polyploidized cells of *Allium cepa* exposed to trifluralin herbicide. *Pestic Biochem Physiol* **88**:252–259 (2007). <https://doi.org/10.1016/j.pestbp.2006.12.003>.

62 Monarca S, Feretti D, Collivignarelli C, Guzzella L, Zerbini I, Bertanza G *et al.*, The influence of different disinfectants on mutagenicity and toxicity of urban wastewater. *Water Res* **34**:4261–4269 (2000). [https://doi.org/10.1016/S0043-1354\(00\)00192-5](https://doi.org/10.1016/S0043-1354(00)00192-5).

63 Feng S, Hao Ngo H, Guo W, Woong Chang S, Duc Nguyen D, Cheng D *et al.*, Roles and applications of enzymes for resistant pollutants removal in wastewater treatment. *Bioresour Technol* **335**:125278 (2021). <https://doi.org/10.1016/j.biortech.2021.125278>.